ACS NANO

www.acsnano.org

ARTICLE

Nanoscale Venturi–Bernoulli Pumping of Liquids

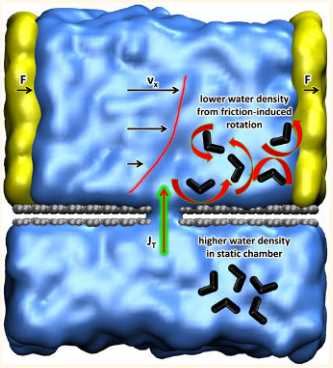
Pavel Rehak,[‖] Haiqi Gao,[‖] Ruifeng Lu, and Petr Král*

Cite This: *ACS Nano* 2021, 15, 10342–10346

Read Online

ACCESS | Metrics & More | Article Recommendations | Supporting Information

ABSTRACT: **We use molecular dynamics simulations to show that the Venturi–Bernoulli effect can pump liquids at the nanoscale. In particular, we found that water flowing in an open reservoir close to a static substrate experiences a friction which converts its kinetic energy into breaking of hydrogen bonds. This water flowing under friction acquires a lower density, which can be used in pumping fluids positioned under a nanoporous substrate.**



KEYWORDS: *liquid pumping, Venturi–Bernoulli effect, molecular dynamics simulations, nanofluidics, motility*

Downloaded via UNIV OF ILLINOIS CHICAGO on July 30, 2021 at 18:42:22 (UTC).
See https://pubs.acs.org/sharingguidelines for options on how to legitimately share published articles.

Nanofluidic devices based on graphene nanopores and related layered materials[1] could be used in desalination,[2] water filtration,[3] and ion separation.[1,4] Water within molecular distances from surfaces flows differently than predicted by classical fluidic models. This is best seen on its flow through nanochannels,[5,6] where a parabolic velocity (cross section) profile of water passing through microchannels, associated with a Poiseuille flow, is replaced by a flat velocity profile,[7] due to water slipping on the walls. Therefore, water transport through carbon nanotubes can be 4–5 orders of magnitude faster than predicted by classical fluid flow models.[8]

The pressure of liquids passing through channels is correlated with their velocity when the channel cross sections are gradually changed (Venturi 1799). This is caused by the conservation of the total (kinetic and potential) energy density (Bernoulli 1738), where individual components are converted into each other like in a spring:

$$\rho v^2/2 + P + P_{\text{shaft}} + P_{\text{loss}} = \text{const} \quad (1)$$

In this equation, ρ is a local mass density of the liquid, v is its local velocity (giving a kinetic energy density, $\rho\, v^2/2$), P is its local pressure (potential energy density), P_{shaft} is a local pressure resulting from external forces driving the liquid, and P_{loss} is the local pressure loss due to friction and other reasons.[9] The Venturi–Bernoulli (VB) effect is used in medicine, measurement of liquid flows, and aviation, but planes flying at very high speeds are supported by a direct transfer of vertical momentum to the air rather than the VB effect.

At nanoscale, where low Reynolds numbers operate, liquids can be pumped by hydrostatic pressures,[1,2] temperature gradients,[10] electric fields,[11] surface waves,[12] and other means.[13] Here, we use molecular dynamics (MD) simulations to investigate the VB effect at the nanoscale and its possible use in liquid pumping. We simulate liquids passing through open channels and study whether their passage around nanoscale slits can pump liquids.

RESULTS AND DISCUSSION

Figure 1a,b shows the two simulated open reservoirs partly filled with flowing (top) and static (bottom) water. The reservoirs are separated by a stacked and fixed two-layer graphene with an ultranarrow slit, aligned in a direction orthogonal to the water flow in the upper chamber. There is free space (filled with water vapor) above the water surfaces in both containers, which is shared in a 3D periodic cell (gravity forces are negligible). Graphene (not shown) is also located in this vapor phase separating the liquid surfaces, so that water can only be pumped through the slit, as a response to water forced to laterally flow in the upper reservoir. Water is

Received: March 25, 2021
Accepted: May 19, 2021
Published: May 24, 2021



© 2021 American Chemical Society

https://doi.org/10.1021/acsnano.1c02557
ACS Nano 2021, 15, 10342–10346

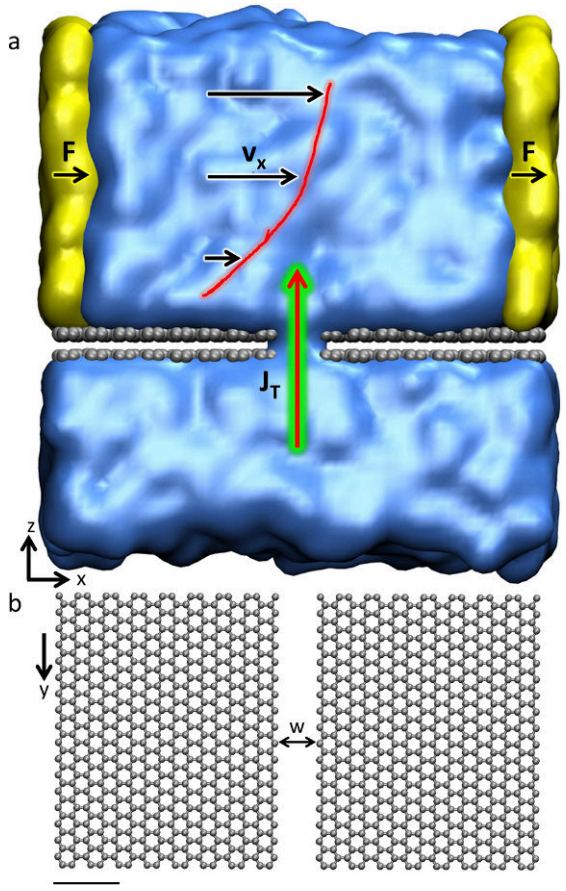


Figure 1. (a) Simulated system of two chambers partly filled with water (blue) and separated by a stacked graphene bilayer with a slit (periodic conditions). In the upper chamber, a force F is applied to water oxygens in the yellow region, causing water to flow with a gradient of velocties v_x, due to friction with graphene. The laterally flowing water in the upper chamber has a decreased density, which pumps water from the bottom chamber with a net flow J_T. (b) Top view of the graphene slit. Scale bar is 1 nm.

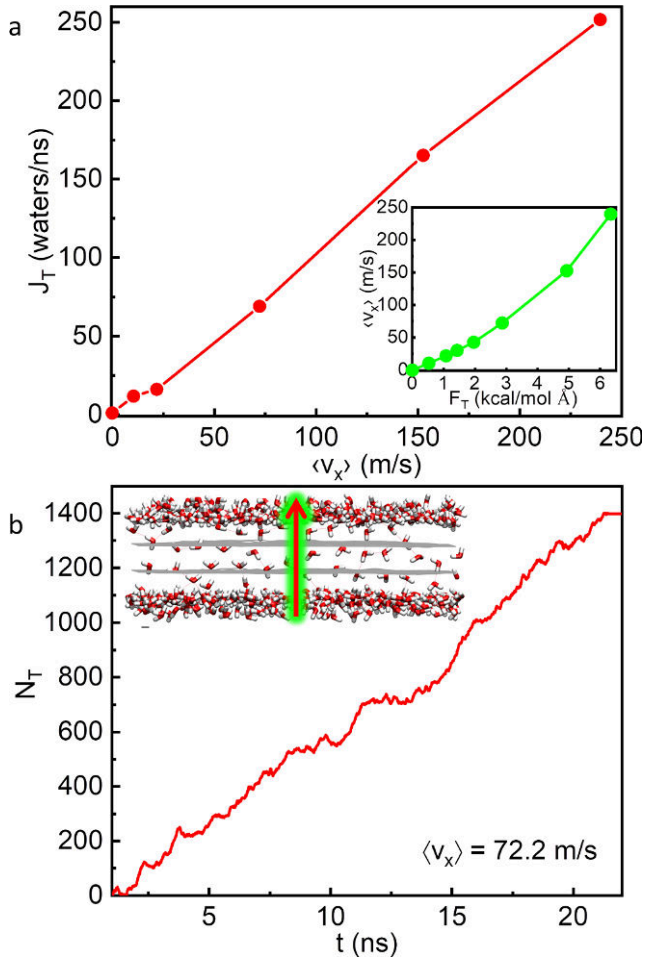


Figure 2. (a) Net water flow through the slit, J_T, obtained for different time-and-space-averaged velocities of water, $\langle v_x \rangle$, laterally flowing in the upper chamber. (Inset) The average velocity of water $\langle v_x \rangle$ in the upper chamber versus the total force, F_T, acting on selected oxygen atoms. (b) The net number of water molecules, N_T, passed up across the slit of w = 0.68 nm width at different times for a water lateral net force of F_T = 2.87 kcal mol^{-1} Å^{-1} (F_x = 7.17 × 10^{-3} kcal mol^{-1} Å^{-1} per molecule), inducing a velocity of $\langle v_x \rangle \approx$ 72.2 m/s in the upper chamber. (Inset) The slit remains filled with water during the pumping. The scale bar is 1 nm.

described by the Newtonian mechanics to avoid its artificial damping by the Langevin dynamics, which is only applied on selected graphene atoms (Methods). This damping should be sufficient to provide cooling of the forced water.

First, water was equilibrated (30 ns), while filling the slit by diffusion,[5,14,15] where it remained during the simulations (Figure 2b (inset)). In equilibrium, both water flows through the slit, $J_{up,down}$, were about the same, giving a zero net flow, $J_T = J_{up} - J_{down} \approx 0$ waters/ns. In order to maintain a steady-state lateral flow of water in the upper chamber, a force F_x oriented along the graphene surface was applied on the oxygen atoms of water molecules at $z > 0$, within 0.3 nm from the $\pm x$ graphene boundaries (yellow region in Figure 1a).[16] The (time and $y - z$-area) averaged induced velocity of molecules $\langle v_x \rangle$ depends on the total force, F_T, applied on all molecules, as shown in Figure 2a (inset). Figure 2a shows the water fluxes through the slit, J_T, induced by laterally flowing water with average velocities of $\langle v_x \rangle$. These results reveal that the simulations are roughly done in a linear regime, despite relatively large water velocities. Figure 2b also shows how water passes in time through the slit for $\langle v_x \rangle$ = 72.2 m/s.

We can check if the water flow (upper chamber) can be described on average by the macroscopic relationship, $\langle v_x \rangle / F_x = nH^2/\eta$, where F_x is the driving force per molecule, $\eta \approx 10^{-3}$ Pa s is the viscosity, H = 7.2 nm is the length of the chamber, and n is the numerical density of water molecules to which force is applied (initially $n \approx$ 2.96 molecules/nm^3 because the force is applied within 6 Å of the 7.2 nm long region). Upon division by the number of dragged molecules, n_{app}, the left side, $\langle v_x \rangle / n_{app}$ $F_x = \langle v_x \rangle / F_T \approx$ 0.329 Å^2 mol/(ps kcal), can be obtained from the linear fit in Figure 2a (inset). The right side, $H^2/\eta V_{chamber} \approx$ 0.381 Å^2 mol/(ps kcal) ($V_{chamber} \approx 7.2 \times 4.1 \times 3.2$ nm^3 = 94.5 nm^3), is in good agreement with the left side, showing that the macroscopic description is on average valid here.

We can further analyze the water flow in the upper chamber by calculating the space-localized and time-averaged velocity components, $\overline{v}_{x,z}$. Using a total driving force of F_T = 2.87 kcal/mol Å, we calculate the velocities at x = 0 nm (above the slit) and $x = \pm$ 1 nm (away from the slit) at different distances z from the surface, as shown by the solid vertical arrows in Figure 3c (inset). Figure 3a reveals that $\overline{v}_x \approx$ 85 m/s at z = 4 nm, but it drops to $\overline{v}_x \approx$ 40 m/s as $z \to 0$, due to friction with

https://doi.org/10.1021/acsnano.1c02557
ACS Nano 2021, 15, 10342−10346

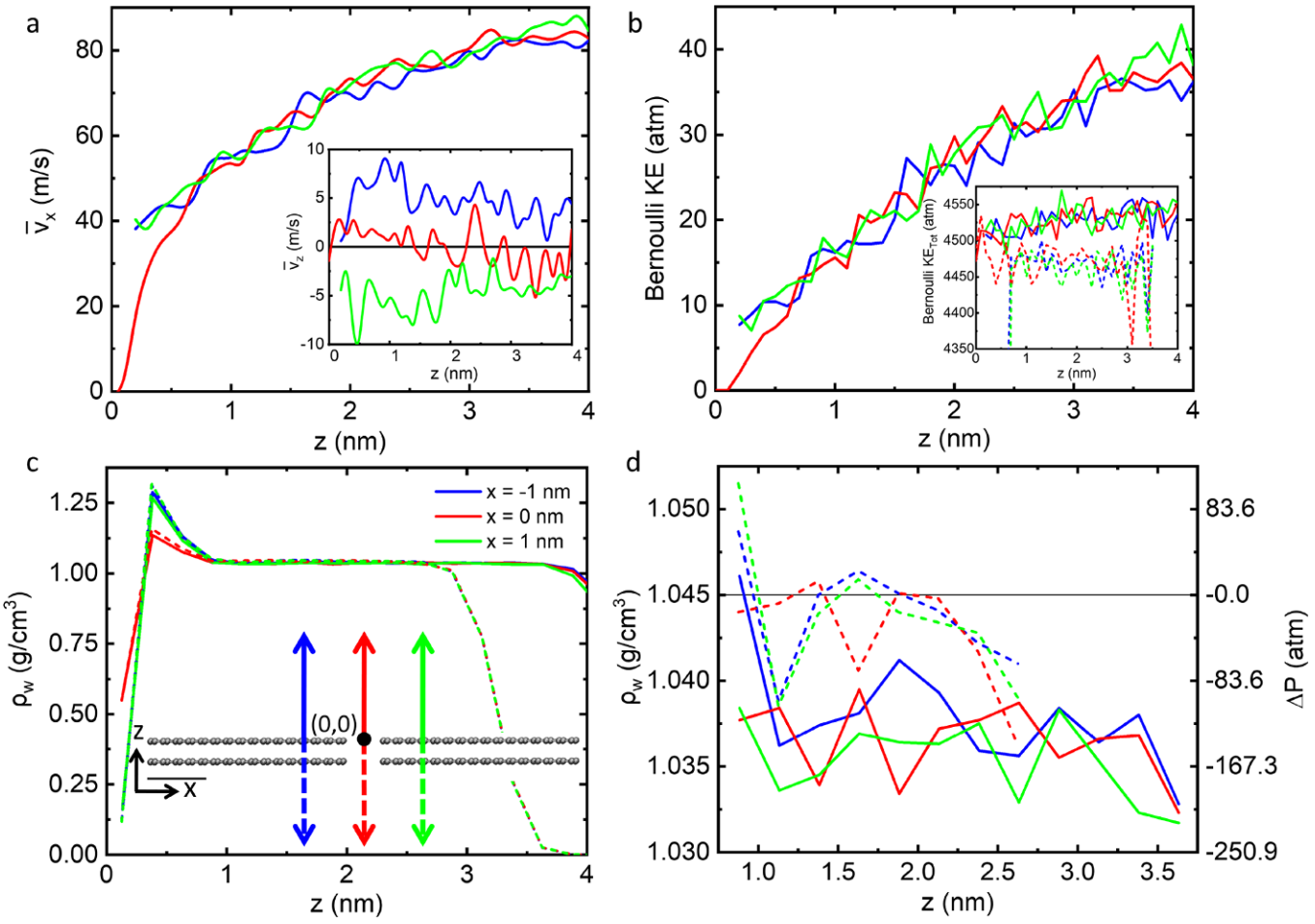


Figure 3. (a) Time-averaged lateral velocities of water, $\overline{v}_x$ and $\overline{v}_z$ (inset), calculated in the upper chamber as a function of distance from graphene (z) and the slit (x) (inset of panel c). A lateral net force of F_T = 2.87 kcal mol^{-1} Å^{-1} is generated by applying $F_x = 7.17 \times 10^{-3}$ kcal mol^{-1} Å^{-1} per water molecule (narrow region). (b) Translational kinetic energy density of water in the dynamic chamber, $P_{KE} = (1/2)\rho_N m_w (\overline{v}_x^2 + \overline{v}_z^2)$, where the number density is $\rho_N \approx 36.1$ molecules/nm^3, m_w is the molecular weight of water, and the velocities are in panel a. (inset) Total kinetic energy density, $P_{KE}^T = \sum_i^{atoms}(1/2)\rho_N m_i(v_{x,i}^2 + v_{y,i}^2 + v_{z,i}^2)$. (c) Mass densities of water calculated at different positions above (solid) and below (dashed) (separate simulation with $F_x = 0$) the graphene layers. (inset) Directions of calculations are shown with arrows separated 1 nm from each other; scale bar is 1 nm. (d) Magnification of panel c. Distances in both chambers are measured from their own graphene surfaces.

the surface, and $\overline{v}_x \approx 0$ above the slit. At distances of $z > 0.5$ nm, $\overline{v}_x$ is very similar at all three positions x. Figure 3a (inset) also shows that water partly moves away from graphene at $x = -1$ nm and returns back at $x = 1$ nm, signifying that the flowing water passed around slow water pumped through the slit.

From these velocity components, we can calculate the translational kinetic energy density of water, $P_{KE} = (1/2)\rho_N m_w(\overline{v}_x^2 + \overline{v}_z^2) = 10-40$ atm ($\rho_N \approx 36.1$ molecules/nm^3 and m_w is the molecular weight of water), shown in Figure 3b (the first term in eq 1). The kinetic energy density, P_{KE}, is relaxed by friction into heat, P_{loss} (the second term in eq 1), which is supposed to grow as z drops. When all kinetic energy components (translation, rotation, vibration) are added, using the actual velocities of all atoms in water, we obtain $P_{KE}^T \approx$ 4525 and 4465 atm in the dynamic and static chambers, respectively (Figure 3b (inset)). The difference of these values (60 atm) is somewhat larger than the excess of P_{KE} (10−40 atm) present in the dynamic chamber. This is caused by the excessive rotation and vibration of water flowing in the upper chamber.

Figure 3c,d also reveals the local mass densities of water, ρ_w, calculated as a function of distance from their own graphene surfaces. In both chambers, $\rho_w \approx 1$ g/cm^3, except for the following: (1) close to graphene ($z \approx 0.5$ nm), where ρ_w is enhanced since water cannot form hydrogen bonds with it and resides in well-defined monolayers (ρ_w is slightly reduced in the slit area, where water bonds are more preserved), and (2) close to the water surface ($z \approx 4$ nm, solid, top; $z \approx 3$ nm, dashed, bottom), where ρ_w drops at the fluctuating water surfaces. Upon magnification of these results, Figure 3d reveals that ρ_w in the dynamic chamber is roughly constant and by $\Delta\rho_w \approx 0.0075$ g/cm^3 *lower* than in the static chamber. The reduced density of flowing water is caused by friction, which breaks its hydrogen bonds and forms nanoscopic bubbles. It is also responsible for the pumping of water from the static to the dynamic chamber (see Supporting Information movie (20 ns) for the system in Figure 2b).

However, we cannot directly relate this reduced non-equilibrium density of water to its pressure (state variable), since bubbles should be formed in equilibrium water at such a density (two-phase system). To gain a qualitative picture, we can assign the effective pressure drop between the two

https://doi.org/10.1021/acsnano.1c02557
ACS Nano 2021, 15, 10342−10346

chambers to values obtained from a linear relationship between density and pressure, $dP/d\rho = 1.7 \times 10^4$ atm cm^3/g, which is, however, only valid for water compression.[17] Using this relationship also for water dilution (extrapolation) and assuming that the static chamber has a zero water pressure ($\rho_w \approx 1.045$ g/cm^3), we can obtain in the dynamic chamber an effective (negative) drop in pressure of $\Delta P \approx -120$ atm, as shown in Figure 3d (right axis).

CONCLUSIONS

In summary, our simulations show that the Venturi−Bernoulli effect operates at nanoscale. In the dynamic chamber of the present system, the density (effective pressure P) of flowing water drops due to friction, which allows pumping of water between the static and dynamic chambers. The VB effect could be further explored in nanoscale channels with narrowed regions, where a mutual conversion of kinetic and potential energies can be studied. It could be used in pumping of liquids, measuring of pressures, separations of molecules, and propelling of nanosystems.

METHODS

MD simulations were done with NAMD,[18] using a CHARMM force field[19] and the TIP3P water.[20] The Langevin dynamics was used with a damping constant of $\gamma = 1$ ps^{-1} on only graphene atoms that did not border the periodic edges. The graphene atoms that bordered the edges were held fixed. Water molecules were described through pure Newtonian mechanics. The time step was set to 2 fs. The *NVT* ensemble was used at a temperature of $T = 298$ K. The particle mesh Ewald (PME) summation was used to describe long-range coulombic interactions in the presence of periodic boundary conditions.[21] The switching distance for nonbonded interactions was set to $r_{on} = 8$ Å, and the cutoff was set to $r_{off} = 10$ Å. The positions and velocity components were recorded every 10 ps for the entire trajectory.

In Figures 2 and 3, $\overline{v}_i$ is the ith component of water oxygen velocity averaged over all times (and a spacial element of $\Delta x = 1$ nm, $\Delta z = 1.0$ nm, and whole y axis), while $\langle v_i \rangle$ is $\overline{v}_i$ averaged also over the entire chamber. The water densities (velocities) were determined at $x = 0$, ± 1 nm, $\Delta x = 1$ nm, $\Delta z = 0.25$ (0.1) nm, and averaged over the entire y axis. The flow rates between different chambers were determined from the positions of oxygen atoms in neighboring snapshots. Velocities to determine kinetic energy within the same chamber were determined directly from the NAMD trajectory.

ASSOCIATED CONTENT

Supporting Information

The Supporting Information is available free of charge at https://pubs.acs.org/doi/10.1021/acsnano.1c02557.

> Movie showing MD simulation (20 ns) of the system in Figure 1, where a net force of $F_T = 2.87$ kcal mol^{-1} Å^{-1} induced a water velocity of $\langle v_x \rangle \approx 72.2$ m/s in the upper chamber, with the transfer of water from the bottom chamber to the upper chamber clearly seen (AVI)

AUTHOR INFORMATION

Corresponding Author

Petr Král − *Department of Chemistry and Departments of Physics, Pharmaceutical Sciences, and Chemical Engineering, University of Illinois at Chicago, Chicago, Illinois 60607, United States;* orcid.org/0000-0003-2992-9027; Email: pkral@uic.edu

Authors

Pavel Rehak − *Department of Chemistry, University of Illinois at Chicago, Chicago, Illinois 60607, United States*

Haiqi Gao − *Department of Chemistry, University of Illinois at Chicago, Chicago, Illinois 60607, United States; Department of Applied Physics, Nanjing University of Science and Technology, Nanjing 210094, People's Republic of China*

Ruifeng Lu − *Department of Applied Physics, Nanjing University of Science and Technology, Nanjing 210094, People's Republic of China;* orcid.org/0000-0002-1752-2070

Complete contact information is available at: https://pubs.acs.org/10.1021/acsnano.1c02557

Author Contributions

‖P.R. and H.G. contributed equally.

Notes

The authors declare no competing financial interest.

ACKNOWLEDGMENTS

This work is dedicated to Margareta L. F. Rehak.

REFERENCES

(1) Sint, K.; Wang, B.; Král, P. Selective Ion Passage through Functionalized Graphene Nanopores. *J. Am. Chem. Soc.* **2008**, *130*, 16448−9.

(2) Cohen-Tanugi, D.; Grossman, J. C. Water Desalination across Nanoporous Graphene. *Nano Lett.* **2012**, *12*, 3602−8.

(3) Gopinadhan, K.; Hu, S.; Esfandiar, A.; Lozada-Hidalgo, M.; Wang, F. C.; Yang, Q.; Tyurnina, A. V.; Keerthi, A.; Radha, B.; Geim, A. K. Complete Steric Exclusion of Ions and Proton Transport through Confined Monolayer Water. *Science* **2019**, *363*, 145−148.

(4) Abraham, J.; Vasu, K. S.; Williams, C. D.; Gopinadhan, K.; Su, Y.; Cherian, C. T.; Dix, J.; Prestat, E.; Haigh, S. J.; Grigorieva, I. V.; Carbone, P.; Geim, A. K.; Nair, R. R. Tunable Sieving of Ions Using Graphene Oxide Membranes. *Nat. Nanotechnol.* **2017**, *12*, 546−550.

(5) Hummer, G.; Rasaiah, J. C.; Noworyta, J. P. Water Conduction through the Hydrophobic Channel of a Carbon Nanotube. *Nature* **2001**, *414*, 188−90.

(6) Suk, M. E.; Aluru, N. R. Water Transport through Ultrathin Graphene. *J. Phys. Chem. Lett.* **2010**, *1*, 1590−1594.

(7) Joseph, S.; Aluru, N. R. Why Are Carbon Nanotubes Fast Transporters of Water? *Nano Lett.* **2008**, *8*, 452−458.

(8) Majumder, M.; Chopra, N.; Andrews, R.; Hinds, B. Nanoscale Hydrodynamics: Enhanced Flow in Carbon Nanotubes. *Nature* **2005**, *438*, 44−44.

(9) Blocken, B.; Moonen, P.; Stathopoulos, T.; Carmeliet, J. Numerical Study on the Existence of the Venturi Effect in Passages between Perpendicular Buildings. *J. Eng. Mech.* **2008**, *134*, 1021−1028.

(10) Longhurst, M. J.; Quirke, N. Temperature-Driven Pumping of Fluid through Single-Walled Carbon Nanotubes. *Nano Lett.* **2007**, *7*, 3324−8.

(11) Rinne, K. F.; Gekle, S.; Bonthuis, D. J.; Netz, R. R. Nanoscale Pumping of Water by AC Electric Fields. *Nano Lett.* **2012**, *12*, 1780−3.

(12) Insepov, Z.; Wolf, D.; Hassanein, A. Nanopumping Using Carbon Nanotubes. *Nano Lett.* **2006**, *6*, 1893−5.

(13) Král, P.; Wang, B. Material Drag Phenomena in Nanotubes. *Chem. Rev.* **2013**, *113*, 3372−3390.

(14) Pascal, T. A.; Goddard, W. A.; Jung, Y. Entropy and the Driving Force for the Filling of Carbon Nanotubes with Water. *Proc. Natl. Acad. Sci. U. S. A.* **2011**, *108*, 11794−8.

(15) Cambre, S.; Schoeters, B.; Luyckx, S.; Goovaerts, E.; Wenseleers, W. Experimental Observation of Single-File Water Filling

of Thin Single-Wall Carbon Nanotubes Down to Chiral Index (5,3). *Phys. Rev. Lett.* **2010**, *104*, 207401.
(16) Li, W.; Wang, W. S.; Zhang, Y. N.; Yan, Y. G.; Dai, C. L.; Zhang, J. Gated Water Transport through Graphene Nanochannels: From Ionic Coulomb Blockade to Electroosmotic Pump. *J. Phys. Chem. C* **2017**, *121*, 17523−17529.
(17) Ghodsi, S. M.; Sharifi-Asl, S. S.; Rehak, P.; Král, P.; Megaridis, C. M.; Shahbazian-Yassar, R.; Shokuhfar, T. Assessment of Pressure and Density of Confined Water in Graphene Liquid Cells. *Adv. Mater. Interfaces* **2020**, *7*, 1901727−1901736.
(18) Phillips, J. C.; Braun, R.; Wang, W.; Gumbart, J.; Tajkhorshid, E.; Villa, E.; Chipot, C.; Ske el, R. D.; Kalé, L.; Schulten, K. Scalable Molecular Dynamics with NAMD. *J. Comput. Chem.* **2005**, *26*, 1781−1802.
(19) MacKerell, A. D.; Bashford, D.; Bellott, M.; Dunbrack, R. L.; Evanseck, J. D.; Field, M. J.; Fischer, S.; Gao, J.; Guo, H.; Ha, S.; Joseph-McCarthy, D.; Kuchnir, L.; Kuczera, K.; Lau, F. T. K.; Mattos, C.; Michnick, S.; Ngo, T.; Nguyen, D. T.; Prodhom, B.; Reiher, W. E.; et al. All-Atom Empirical Potential for Molecular Modeling and Dynamics Studies of Proteins. *J. Phys. Chem. B* **1998**, *102*, 3586−3616.
(20) Jorgensen, W. L.; Chandrasekhar, J.; Madura, J. D.; Impey, R. W.; Klein, M. L. Comparison of Simple Potential Functions for Simulating Liquid Water. *J. Chem. Phys.* **1983**, *79*, 926−935.
(21) Essmann, U.; Perera, L.; Berkowitz, M. L.; Darden, T.; Lee, H.; Pedersen, L. G. A Smooth Particle Mesh Ewald Method. *J. Chem. Phys.* **1995**, *103*, 8577−8593.

https://doi.org/10.1021/acsnano.1c02557
ACS Nano 2021, 15, 10342−10346